Northeastward growth and uplift of the Tibetan Plateau: Magnetostratigraphic insights from the Guide Basin

Josep M. Pares,[1] Rob Van der Voo,[1] Will R. Downs,[2] Maodu Yan,[1] and Xiaomin Fang[3]

Received 24 September 2001; revised 9 April 2002; accepted 24 June 2002; published 11 January 2003.

[1] Most of the evidence for the uplift of the Tibetan Plateau comes from its southern and central parts. Although the northern rim has been less studied, it may greatly contribute to the understanding of the mechanism and timing of the uplift. Recent studies on the northeastern part of the plateau suggest that the uplift can largely be explained by Cenozoic thrusting and folding linked to the movement of the Altyn Tagh and Kunlun faults and that diffuse shortening might be a realistic way to explain the thickening of the continental interior. Nevertheless, the age of sediments that record the tectonic processes is poorly known. The terrigenous formations in the Guide–Gonghe Basin, NE Tibet, show several phases of deformation and include thick deposits of conglomerates, interbedded with sandstones and siltstones that are thought to be the result of an increased sediment flux. Dating of these gravel deposits with magnetostratigraphic and faunal studies has permitted the precise timing of the basin infilling and its tectonic evolution to be established. Our results indicate that the onset of conglomerate accumulation occurs in the Pliocene, an observation that is in agreement with those of the Linxia Basin, just east of the Plateau. If the high sedimentation rates (~22 cm/kyr) in the Guide Basin are mostly due to tectonism, then significant uplift occurred as late as Pliocene. *INDEX TERMS:* 1520 Geomagnetism and Peleomagnetism: Magnetostratigraphy; 8102 Tectonophysics: Continental contractional orogenic belts; 9320 Information Related to Geographic Region: Asia; 9604 Information Related to Geologic Time: Cenozoic

Citation: Pares, J. M., R. Van der Voo, W. R. Downs, M. Yan, and X. Fang, Northeastward growth and uplift of the Tibetan Plateau: Magnetostratigraphic insights from the Guide Basin, *J. Geophys. Res.*, *108*(B1), 2017, doi:10.1029/2001JB001349, 2003.

1. Introduction

[2] After the Indian and Eurasian continents began colliding in the Paleogene, continued convergence in central Asia produced the Himalayan–Tibetan orogen, one of the most spectacular geologic features on Earth. Most of the Indo-Asian convergence has been taken up by large-scale thrusting within the Himalayas and by major strike-slip faulting accommodated within and around the Tibetan Plateau. Half of the current rate of convergence between India and Asia, as shown by GPS measurements [*Chen et al.*, 2000; *Holt et al.*, 2000; *Wang et al.*, 2001] is taken up in the Himalayas [*Lyon-Caen and Molnar*, 1985; *Burchfiel and Royden*, 1991]. Extrapolating this shortening to the geologic past requires that the other half of the convergence must have been accommodated within and around the margins of the Tibetan Plateau [*Royden and Burchfiel*, 1997]. The Tibetan Plateau is thus an unprecedented area for furthering the understanding of the processes of intracontinental deformation and its relation to uplift.

[3] The pattern of deformation and present rates of convergence in the Himalayan–Tibetan orogen suggest that the Tibetan Plateau has been growing northward during the late Cenozoic, but confirmation of this requires more studies in the northern part of the plateau. So far, the views on Cenozoic tectonic evolution of NE Tibet remain controversial, largely due to a scarcity of basic geologic data, including the age of the sedimentary infilling in the basins within the Plateau.

[4] The geologic features of NE Tibet include two major fault systems, Qilian and Kunlun (Figure 1). The structural features between these two systems suggest a young northward growth of the Tibetan Plateau in the Cenozoic [e.g., *Tapponnier et al.*, 1990; *Burchfiel and Royden*, 1991; *Métivier et al.*, 1998]. Indeed, recent studies on the Qaidam Basin and its surroundings [*Tapponnier et al.*, 1990; *Meyer et al.*, 1998; *Métivier et al.*, 1998] indicate that the main morphotectonic units in northern Tibet can largely be explained by Late Tertiary thrusting and folding linked to movement along the Altyn Tagh and Kunlun faults. In this scenario, the NW–SE trending mountain ranges are explained as large-scale ramp anticlines, whereas the intramontane depressions (e.g. Qaidam basin) are piggyback basins caught between the rising ranges [*Métivier et al.*, 1998].

[1]Department of Geological Sciences, University of Michigan, Ann Arbor, Michigan, USA.
[2]Department of Geology, Northern Arizona University, Flagstaff, Arizona, USA.
[3]Department of Geography, Lanzhou University, China.

0148-0227/03/2001JB001349$09.00

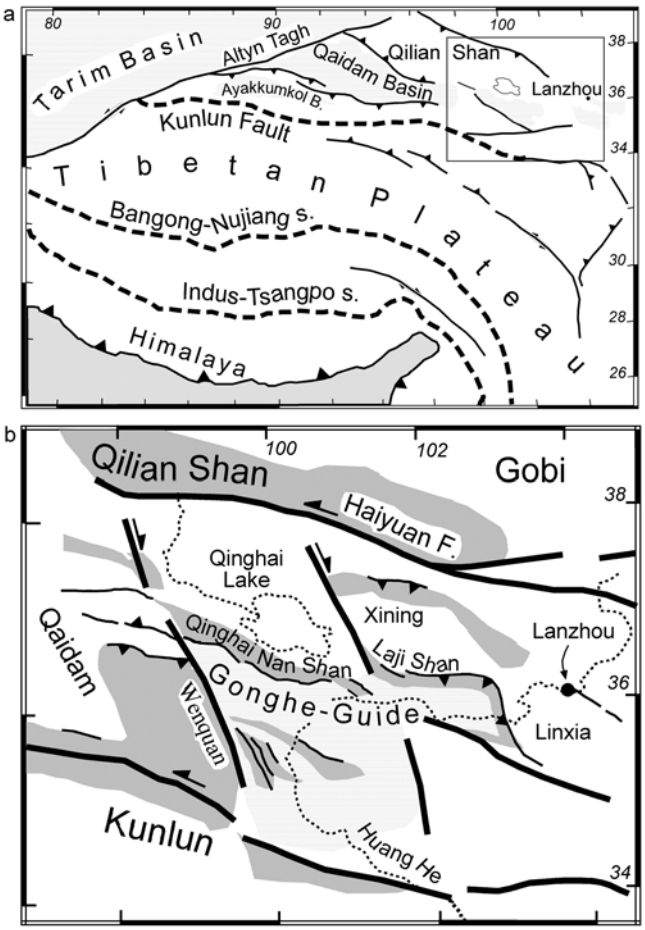

Figure 1. (a) Regional map of the Tibetan Plateau and (b) schematic tectonic map of the area around Guide showing the major structural features, mountain ranges (dense stipple) and the Gonghe–Guide Basin (light stipple). Modified from *Qinghai Geology Bureau* [1972], *Meyer et al.* [1998], and *Yin and Harrison* [2000].

[5] Most recent tectonic studies have focused on the northern margin of Tibet and the relations between the Altyn Tagh fault and fold and thrust structures adjacent to the Qaidam Basin and within the NW Qilian Shan [e.g. *Burchfiel et al.*, 1989; *Tapponnier et al.*, 1990; *Wang*, 1997]. With the exception of the study on the Haiyuan fault and related structures by *Zhang et al.* [1991], *Burchfiel et al.* [1991] and *Meyer et al.* [1998], little work has been done in the northeastern part of the Tibetan Plateau. We report here a study focused on determining the age of sedimentation in the Guide Basin, which is located between the Kunlun and Haiyuan fault systems (Figure 1). This area comprises typical structural features for northern Tibet and, if accurately dated, could yield information on the evolution of the NE part of the Tibetan Plateau during the Neogene. We think that the Kunlun fault system might have been reactivated in the uppermost Miocene–Pliocene and that deformation along the margins of NE Tibet can largely be explained by a transpressional setting, where thrusts coalesce with the major strike-slip faults (Kunlun and Qilian-Haiyuan). A similar model was previously proposed by *Burchfiel and Royden* [1991] for the Altyn Tagh and Qilian Shan region. Extrapolating the current slip rate (~13 mm/yr [*van der Woerd et al.*, 1998]), *Yin and Harrison* [2000] speculate that the Kunlun fault has been active over the past 7 My but more data are needed to establish precise timing. Thus, determining the age of basin initiation in the area of Gonghe–Guide will also provide time constraints on the activity of the Kunlun fault system, an important structural feature related to Neogene deformation and uplift in NE Tibet.

[6] The Guide Basin lies directly north of the Kunlun fault system and south of the Qilian Shan (Figure 1). The Kunlun fault system appears to have played a major role not only during the Indo-Asian collision but also earlier during the Mesozoic evolution of Asia [e.g. *Yin and Harrison*, 2000], as evidenced by Triassic flysch and arc magmatism along the Kunlun suture. Unfortunately, little is known regarding the precise timing of activity along the Kunlun fault during the Tertiary. Because there are no Cenozoic metamorphic rocks, the onset of deformation must be primarily constrained by magnetostratigraphic data of adjacent basins related to the major fault systems (e.g., Gonghe–Guide Basin, Figure 1b). Several Tertiary basins adjacent to the Kunlun and Qilian Shan ranges have been paleomagnetically studied: the Linxia Basin [*Li et al.*, 1997a, 1997b], the Lanzhou basin [*Flynn et al.*, 1999] and the Qaidam basin [*Liu et al.*, 1998; *Dupont-Nivet et al.*, 2002]. On a broader scale, magnetostratigraphy has been extensively used to date Tertiary basins elsewhere in the Tibetan Plateau [e.g. *Harrison et al.*, 1993; *Li et al.*, 1998; *Garzione et al.*, 2000].

[7] We have selected the area of Guide as it is one of the major basins in the region that has been incised to its basement by the Yellow River and its tributaries. Moreover, Pleistocene river erosion has produced steep walled gorges that cut across basin margin ranges exposing basin infill and bounding structures.

2. Geologic Setting

[8] The Gonghe–Guide Basin has an extent of about 40,000 km^2 and is separated from the Qaidam Basin to the W by the NW–SE trending Wenquan fault (Figure 1b). Elevations in the basin range from 2,200 m (base level of Huang He or Yellow River) in the town of Guide to around 5,000 m (highest peaks, consisting of basement rocks). Near the central part of the basin, the Tertiary sedimentary infilling reaches elevations of up to 3,300 m. Incision of the Yellow River has produced two spectacular gorges along its way through the Gonghe–Guide Basin. To the West, the Longyang Gorge (Figure 2), which cuts more than 800 m into bedrock, allows a geographic distinction between the Gonghe and Guide Basins, although both show very similar structural and sedimentary characteristics. To the east, the Yellow River excavates the bedrock at the Songba gorge (Figure 2). To the north, the basin is bordered by the foothills of the Qinghai Nan Shan and Laji Shan, and to the south by the Kunlun range (Figure 1b). NW–SE and E–W faults bound the basin and give rise to its conspicuous rhomboid shape (Figure 1).

[9] The bulk of the Cenozoic sedimentary infilling of the Guide Basin has been informally called ''Guide formation'' [*Qinghai Geology Bureau*, 1972; *Zhai and Cai*, 1984; *Pan et al.*, 1990], a typical molasse as described by *Miall* [1978]. The Guide formation not only records the tectonic history of this portion of the NE Tibetan Plateau but also records the

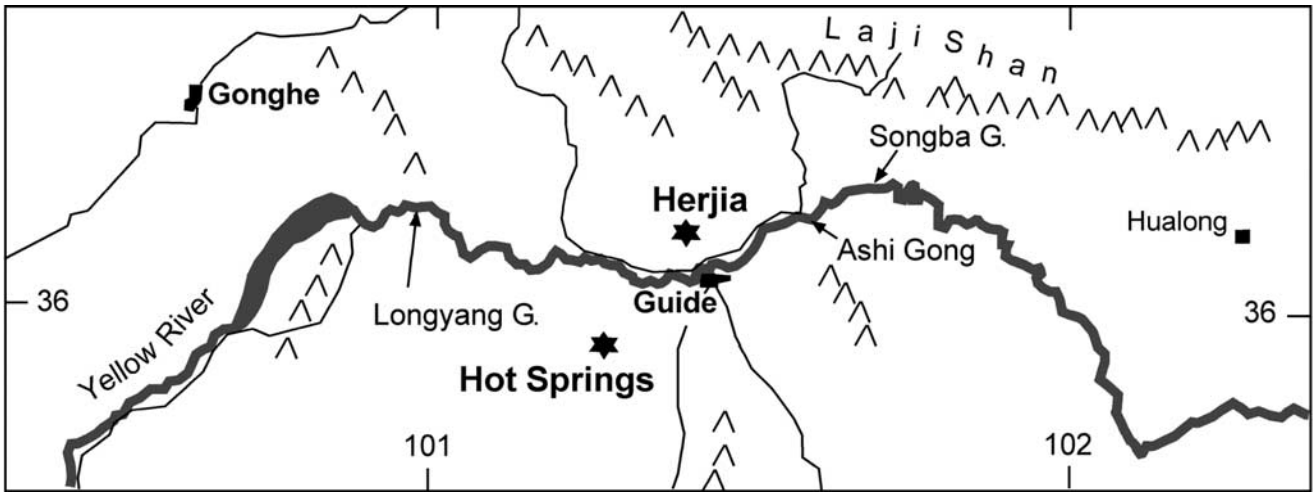

Figure 2. Location map of the Yellow River near the town of Guide, showing the geographic names referred to in the text, including the studied stratigraphic profiles sampled for paleomagnetic analysis (Herjia and Hot Springs).

evolution of the upper section of the Yellow River. The Guide formation is mainly composed of grayish siltstones and pebbly sandstones that are often cross-bedded. The fine-grained sediments of the Guide formation have been interpreted as lacustrine, whereas the gravelly sands are thought to have been deposited in perennial braided-river environments [*Fothergill and Ma*, 1999]. An assemblage of aquatically adapted faunal forms [*Pan*, 1994] indeed shows that the Guide formation was deposited predominantly under the influence of an extensive aquatic environment. *Fothergill* [1998] notes that some sedimentologic properties, namely the mean grain size and sorting of the siltstones, resemble lacustrine deposits from high-energy, semiarid locations in the Karakoram Mountains [e.g. *Owen*, 1996]. Other characteristics include coarse trough cross-bedded sand and gravels, and pebbly sand and local lateral accretion elements, collectively suggestive of a succession of lacustrine and perennial braided river environments. Lacustrine deposits in such environments are thought to be the result of ice or debris flows that temporarily dam the drainage systems [*Owen*, 1996]. Overall, the widespread exposure of thick lacustrine deposits in the Guide Basin suggests that they are products of more long-term, relatively deep-water conditions [*Fothergill*, 1998].

[10] Our preliminary geologic observations along the northern margin of the basin indicate that the Guide formation becomes a thick unit (>800m) of gravels and coarse sandstones, both laterally and upwards. This clastic sedimentary unit, which we informally call ''Ganjia conglomerate'', is well exposed along the foothills of Laji Shan, north of the Guide Basin.

[11] A detailed chronology for the sedimentary infilling of the Cenozoic basins in the Tibetan Plateau is critical as the sediments record the tectonic and climatic evolution of the Plateau. Therefore, making a high-resolution chronostratigraphy of the Guide Basin is our primary goal. All available chronologic information so far is from fossil assemblages. The faunistic associations [*Zheng et al.*, 1985; *Yu et al.*, 1992] collectively indicate that the main part of the western Guide Basin sediments is younger than the Baodean Chinese Age, which is equivalent to the Late Miocene [*Qiu and Qiu*, 1995; *Flynn*, 1997]. Of particular interest are fragments of the proboscidean *Anancus sinensis*, found in the upper part of the Herjia section (Figure 2), along with the rodent *Myospalax arvicolinus* [*Zheng et al.*, 1985], both common in the Pliocene Yushean fauna. The presence of *Hipparion fossatum* at Ashi Gong (east part of the Guide Basin, Figure 2) in the lowermost parts of the sedimentary infill, is characteristic of the Late Miocene [*Pan*, 1994], but this age needs to be confirmed by magnetic stratigraphy. Overall, the biostratigraphic association in Guide is younger than those of other well-dated localities east of Guide including the Linxia [*Li et al.*, 1997a] and Lanzhou [*Flynn et al.*, 1999] basins.

[12] The Guide formation has received a lot of attention for more than seventy years. In the literature, it has been indiscriminately used as a system, formation and even as a group [*Gu et al.*, 1992]. In addition, stratigraphic correlations between different Tertiary basins in NE Tibet (Linxia, Xining, Guide Basins, see Figure 1b) have been attempted using lithostratigraphic criteria. These attempts in correlating Neogene formations between basins have only succeeded in increasing the confusion about the precise stratigraphic position and age of the Guide formation. In the latest publication on Neogene subdivision in the Qinghai Province, the Guide formation is actually considered as a group which is subdivided into three formations (Shangtan, Xiadongshan and Charang formations [*Gu et al.*, 1992]). Nonetheless, we prefer a more general and conservative view and will simply use the informal term of Guide formation for the bulk of the sedimentary infilling in the area of Guide containing a Yushean Fauna. The faunal association (Table1) will allow us to anchor the obtained magnetic polarity to the Geomagnetic Polarity Timescale (CK95 [*Cande and Kent*, 1995]), as discussed below.

3. Magnetic Stratigraphy

[13] Two stratigraphic sections encompassing the lower part of the Guide formation have been paleomagnetically studied. The section referred to as Hot Springs is located

Table 1. Summary of Fossil Assemblages in the Guide Basin (Data From *Zheng et al.* [1985], *Gu et al.* [1992], and *Pan* [1994])

Fossils	Formation	Biochron	Epoch	Location
Anancus sinensis, *Axis shansius*, *Gazella kueitensis*, *Mimomys* sp., *Ochotona* sp., *Hipparion* sp., *Chilotherium* sp., *Gazella kueitensis*	Guide	Yushean	Pliocene	Erdaogou (Herjia Temple)
Myospalax arvicolinus	Guide	Yushean	Pliocene	Rishugou
Hipparion fossatum, Hipparion cf., *platyodus*, *Gomphotherium* sp., *Palaeotragus* sp., *Axis* sp., *Gyraulus* sp., *Pupilla* sp.	Xiadongshan	Baodean	Miocene	Ashigong

SW of the town of Guide and is 140 m thick (Figure 2). The Herjia section, 200 m thick, is north of Guide and takes its name from the temple that is located at the base of the section (base at 2260 m). *Zheng et al.* [1985] studied the fossils along the Herjia profile and these are listed in Table 1.

[14] At each sampling site, one or two large (about 800 cc) oriented blocks were collected from which two or three cubic or cylindrical samples were obtained. All samples were thermally demagnetized and their magnetization measured using a 2G cryogenic magnetometer housed in a shielded room at the University of Michigan. Samples were progressively demagnetized in eleven or more steps up to 680°C or until the intensity became close to the noise level of the cryogenic magnetometer. Representative thermal demagnetization diagrams (Figure 3) show that samples contain two magnetization components. A low unblocking temperature component is commonly removed around 200–300°C. This low-temperature component typically is aligned with the present-day geomagnetic field and is better defined in samples having a reverse polarity high-temperature component (Figure 3). Maximum unblocking temperatures suggest the presence of both magnetite and hematite in the studied rocks. In order to qualitatively estimate the presence of these minerals, a set of IRM acquisition and backfield DC demagnetization curves have been produced (Figure 4). First, we applied a maximum DC field of 1.1 T to the sample. Then, successively increasing fields were applied in the opposite direction, until the saturation IRM is again reached in the opposite sense. The ''back field'' required to reducing the IRM to zero gives the coercivity of maximum remanence [*McElhinny*, 1973], which in our samples is 0.1 to 0.2 T. All measured samples show that more than a half of the initial IRM is reduced at fields of 0.1 T. The S-ratio ($IRM_{-0.3}$/SIRM) [*Stober and Thompson*, 1977] is a convenient measure for discriminating low-coercivity ferromagnetic grains, such as magnetite, from higher coercivity grains such as goethite or hematite. As the proportion of low-coercivity grains saturating in fields less than 0.3 T increases, the S-ratio approaches unity (Figure 4). Overall, our results suggest that a low coercivity phase dominates the NRM and that minor traces of high coercivity phases are present in the studied sediments.

[15] After removal of the partial overprint, a dual polarity Characteristic Remanent Magnetization (ChRM) component is defined in most of the samples. ChRM component directions were calculated for all specimens using Principal Component Analysis [*Kirschvink*, 1980], guided by visual inspection of orthogonal demagnetization plots [*Zijderveld*, 1967]. ChRM directions (Figure 5a) appear to have a more elliptical distribution than the symmetrical distribution required for the application of Fisher statistics. In order to accommodate a non-Fisherian distribution of ChRM vectors, and to characterize the associated uncertainties, we have used the statistical bootstrap technique adapted for paleomagnetic vectors by *Tauxe* [1998]. The bootstrap technique is performed in two steps. First a list of data points is randomly drawn from the original data set using a random number generator to create a ''para-data set''. A mean direction is then calculated for this para-data set. The procedure is then repeated many times by calculating the mean directions for many para-data sets. The region of 95% confidence is delineated by a contour enclosing 95% of the bootstrapped means. Results of bootstrap statistics, including mean directions for both normal and reverse ChRM directions are shown in Figure 5b. Because the ChRM directions are not well fit by a Fisher distribution, the bootstrap statistics that we applied give more appropriate uncertainties for the data distribution.

[16] Both localities (Herjia and Hot Springs) yield positive reversal tests (Figure 5b). We have used the histograms of cartesian coordinates of bootstrapped means to test for a common mean after inverting the reverse directions to their antipode [*Tauxe*, 1998]. The confidence intervals for the different data sets (normal and reverse), shown as horizontal bars in the plots, overlap in all three cartesian components (Figure 5). This observation indicates that the means of normal and reversed directions cannot be distinguished at the 95% level of confidence and hence they pass the bootstrap reversal test.

4. Correlation to the GPTS

[17] Virtual geomagnetic pole (VGP) latitudes are used to illustrate the magnetic polarity of the stratigraphic successions (Figure 6). Both the Herjia and Hot Springs sections are dominantly reversed polarity with the former having three short normal polarity chrons.

[18] The reliability of the obtained magnetic stratigraphy is quantified using the jackknife procedure adapted for magnetostratigraphy by *Tauxe and Gallet* [1991]. The jackknife is a statistical technique that relies on the deletion of data points in order to estimate a parameter of interest. The jackknife adapted for magnetostratigraphy successively deletes greater proportions of the data set (VGP latitudes) and recounts the number of remaining polarity zones. The process is repeated until 20% of the data have been deleted. The average percentage of the polarity zones remaining after each deletion is plotted versus the percentage of sampling sites deleted (Figure 7). The slope of the line

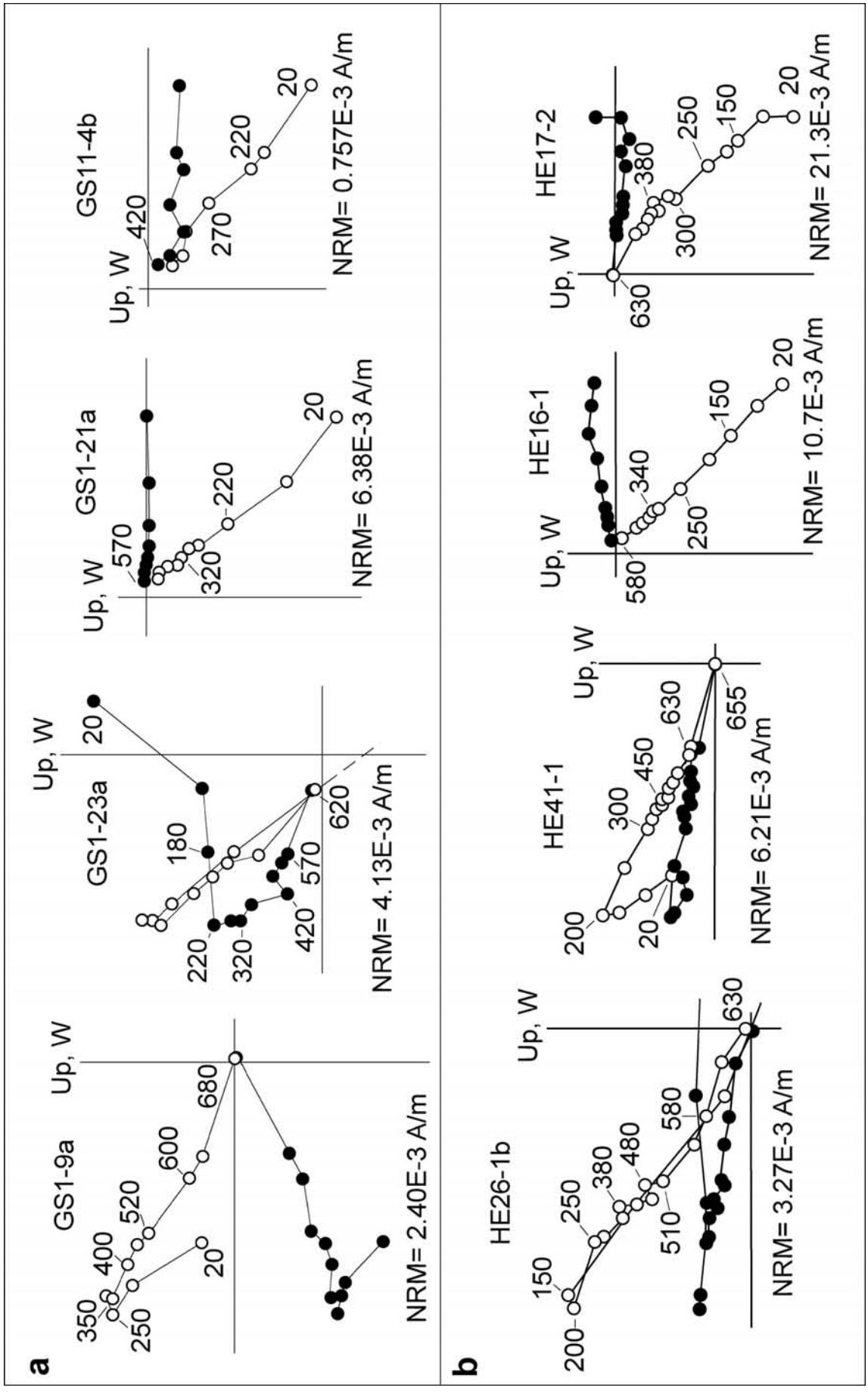

Figure 3. Representative thermal demagnetization diagrams for samples from (a) Hot Springs and (b) Herjia. Closed (open) symbols represent projection of the vector end points onto the horizontal (vertical) plane. Temperatures in Celsius degrees. All plots are in geographic (in situ) coordinates.

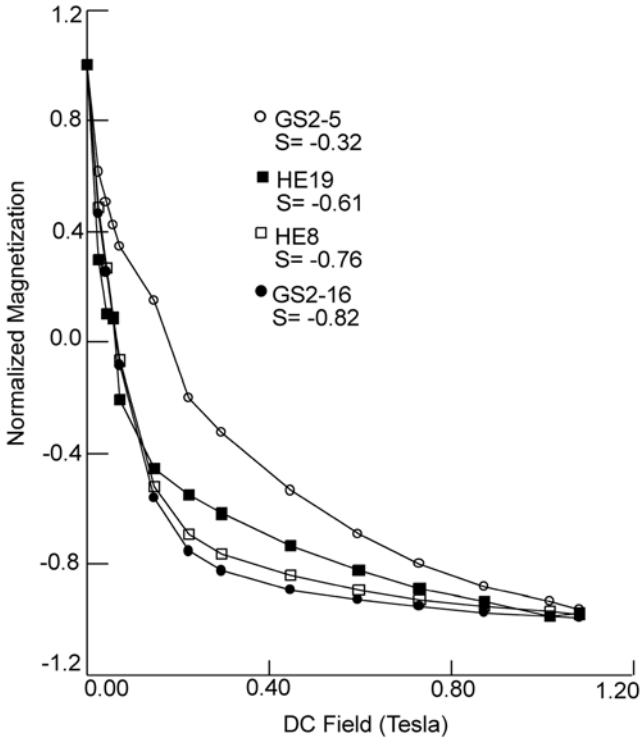

Figure 4. Normalized DC demagnetization curves of Isothermal Remanent Magnetization for representative samples. Samples have been exposed to a field of 1.1 T and a backfield of increasing strength has been subsequently applied. The S-ratio (IRM_{-03}/SIRM) has been determined for each specimen. Note that the S-ratio approaches unity when the proportion of low-coercivity grains saturating in fields less than 0.3 T increases.

generated by this jackknife procedure (called J) is directly related to the sensitivity of the sampled stratigraphy on the particular site distribution [*Tauxe and Gallet*, 1991]. Hence, the value of the jackknife parameter J is a quantitative estimate of the reliability of the sampled section. We applied the jackknife technique (a program by *Tauxe* [1998]) to both Herjia and Hot Springs sections (Figure 7) and the obtained jackknife parameters J have values of -0.43 and -0.25 which would predict that the sections have recovered respectively $\sim$80 and $\sim$90% of the true number of polarity units. We note that *Tauxe and Gallet* [1991], based on numerous simulations, recommend J values in the range of 0 to -0.5 for a robust magnetostratigraphic data set.

[19] The observed magnetic polarity stratigraphy at Herjia can be correlated to the Geomagnetic Polarity Timescale (GPTS) of *Cande and Kent* [1995] (Figure 8). The faunal assemblage in the Herjia section (Table 1) indicates an age equivalent to the Ruscinian for the sediments (Yushean Chinese mammal age). Of particular interest is the genus *Anancus*, which in China is post-Miocene (post-Baodean) and thus requires a younger age than Turolian [*Zheng et al.*, 1985]. The rodents *Myospalax arvicolinus* and Mimomys are also indicative of a Yushean age [*Zheng et al.*, 1985], and rather close to the Villafranchian stage (upper Pliocene). Hence, the observed magnetostratigraphy correlates with the mid Pliocene, around 4 m.y. The three normal polarity chrons as observed in Herjia section ought to correlate with Polarity Chron C3 of the Geomagnetic Polarity Timescale, which includes four normal chrons (Thvera, Sidujfall, Nunivak and Cochiti from bottom to top). The presence of the fossil *Mimomys* in Herjia constrains the age of the bottom of the section, as this rodent is typically not older than the mid-Early Pliocene. Correlating the lowermost normal chron to Thvera subchron would place *Mimomys* at around 4.6 Ma, somewhat older than observed all over Asia [*Qiu and Qiu*, 1995]. We believe that the most plausible interpretation is to consider the lowermost normal chron at Herjia as Sidujfall, which places *Mimomys* and *Myospalax* at around 4 Ma. The observed magnetic polarity most reasonably correlates with the geomagnetic Chron 3n (Gilbert) as shown in Figure 8. The proposed correlation shows that the sediments at Herjia recorded from top to bottom, the Cochiti, Nunivak and Sidufjall subchrons, or Polarity subchrons C3n.1n, C3n.2n and C3n.3n. Hence the studied section at Herjia encompasses about 0.9 m.y. and the suggested correlation to the GPTS yields a bulk accumulation rate of about 22 cm/kyr at Herjia, which is reasonable for such a depositional environment [e.g. *Einsele*, 2000]. The section at Hot Springs has yielded no age-diagnostic fossils so far. Nevertheless, its proximity to the Herjia section, similarity in sedimentary facies and its relative elevation, suggest a possible correlation (Figure 8).

[20] The interpreted magnetic stratigraphy at Herjia has implications for the age of the laterally and upwards equivalent Ganjia conglomerates (Figure 8). Given our stratigraphic age estimate, there is a significant enhancement of denudation in the Pliocene, as indicated by this sudden influx of conglomerates in the Guide Basin.

5. Molasse Sedimentation

[21] One line of evidence for uplift of the Tibetan Plateau derives from its Cenozoic molasse sediments, based on the common belief that the abundance of detrital sedimentary rocks points to nearby source areas of high relief and to enhanced mountain building. Even though climate may strongly influence the availability of gravel-sized material [e.g., *Zhang et al.*, 2001], most studies of geologic formations in well-known foreland basins, such as the Alpine freshwater molasse, Po basin–Adriatic Sea, Ebro Basin, or the Tarim Basin, reveal that thick deposits of detrital sedimentary rocks are intimately related to the tectonic evolution of the margins of the basin and validate the hypothesis of molasse as an orogenic lithostratigraphic unit [e.g., *Einsele*, 2000].

[22] In the Tarim Basin, a thick accumulation of coarse sediments, the Xiyu Formation is widely distributed along the basin's margins and indicates enhanced Pliocene depositional rates that are similar to ours in Guide. Typically, but not exclusively, it comprises a thick accumulation of conglomerate (the "Xiyu gravel" of *Liu et al.* [1996]). Some conglomerates also appear first in the Pliocene outside the Tarim Basin, along the northern and southern margins of the Qilian mountain range. In the vicinity of Yecheng, in the foothills of the western Kunlun Range (southern Tarim Basin), the magnetic stratigraphy of a 2,800 m thick section reveals that the onset of the Xiyu Formation dates back to Chron 2An.3 ($\sim$3.5 Ma), at the base of the Gauss Chron

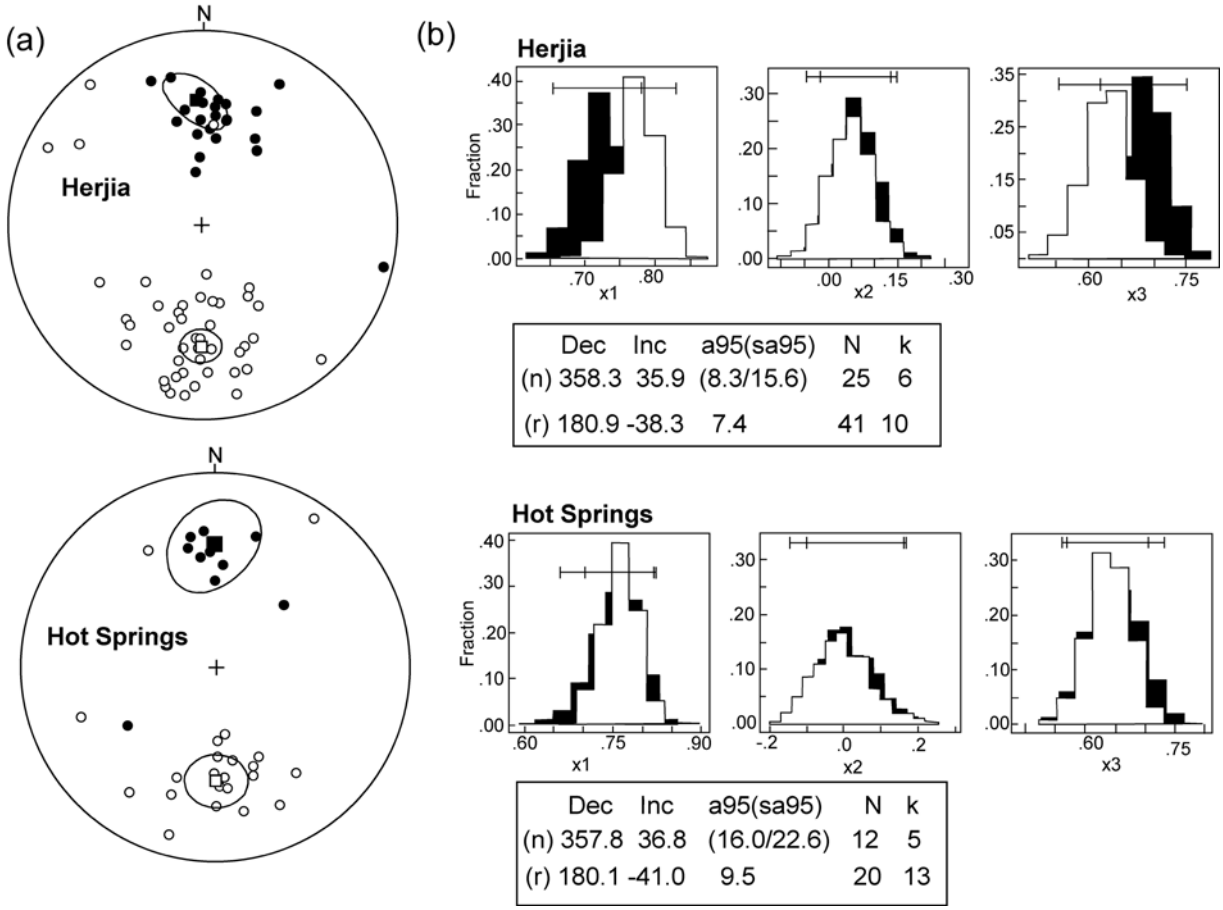

Figure 5. (a) Equal-area projections of the characteristic remanent magnetization (ChRM) directions. Normal (reverse) magnetization directions are shown as dots (open circles). Bootstrap mean directions are indicated by squares with the associated 95% confidence ellipses. (b) Histograms of cartesian coordinates of means of para-data sets drawn from the data shown in (a). The reversed polarity directions have been inverted to their antipodes to test a common mean for the normal (black histogram) and reversed (white histogram) magnetization directions. The confidence intervals for all components overlap, indicating that the two sets of bootstrapped means cannot be distinguished at the 95% level of confidence; they pass the bootstrap reversal test. Dec/Inc—Declination/Inclination; a95/sa95—Radius of the 95% confidence circle/Semiangles of the 95% confidence ellipse (for non-Fisherian distributions).; N—number of samples; k—concentration parameter.

[*Zheng et al.*, 2000]. The underlying sediments, belonging to the Artux Formation, are mostly composed of fine-grained sediments, and locally reach a thickness of 1,000 m [*Zhou and Chen*, 1990]. To a first approximation, the onset of the Xiyu Fm., on top of the Artux Fm., marks an important increase in sedimentation rate and grain size along the margins of the Tarim Basin and Qilian mountains during the upper Pliocene.

[23] The Qaidam basin is a major morphotectonic unit in northern Tibet. It has a mean elevation of 2,700 m and an areal extent of about 100,000 km^2. Several drill logs obtained within the basin have been correlated and studied by *Métivier et al.* [1998] and reveal that the thickness of Pliocene sediments reaches 2,700 m in the eastern margin of the basin. In some drill logs, though lacking a high-resolution chronostratigraphy, the entire Pliocene encompasses up to 1,850 m of molasse sediments. In addition to the presence of thick molasse sediments, Pliocene and Pleistocene increased tectonic activity in the Qaidam basin is also revealed by seismic profiling, as evidenced by folding and thrusting along the Kunlun fault [*Bally et al.*, 1986].

[24] The Linxia basin, south of Lanzhou, is filled by more than 1,600 m of terrigenous and lacustrine sediments and has provided a high-resolution magnetic stratigraphy with an age span from the latest Oligocene to the Pleistocene [*Li et al.*, 1997a]. A relatively thick molasse unit (Jishi Formation) is extensively developed in that basin. The Jishi Formation overlies older formations that contain the well known and rich fossil assemblage of the Longguang fauna, which is characteristic of the Chinese Baodean stage. Magnetic stratigraphy dating at Linxia reveals that the Jishi gravels on top of the Longguang strata are about 3.5 Ma [*Li et al.*, 1997a] and we now document in this study a similar age and increase in coarse clastic sedimentation for the Ganjia conglomerate in the Guide Basin.

[25] Collectively, the Neogene basins in NE Tibet show an increase in rates of terrigenous coarse-clastic sedimenta-

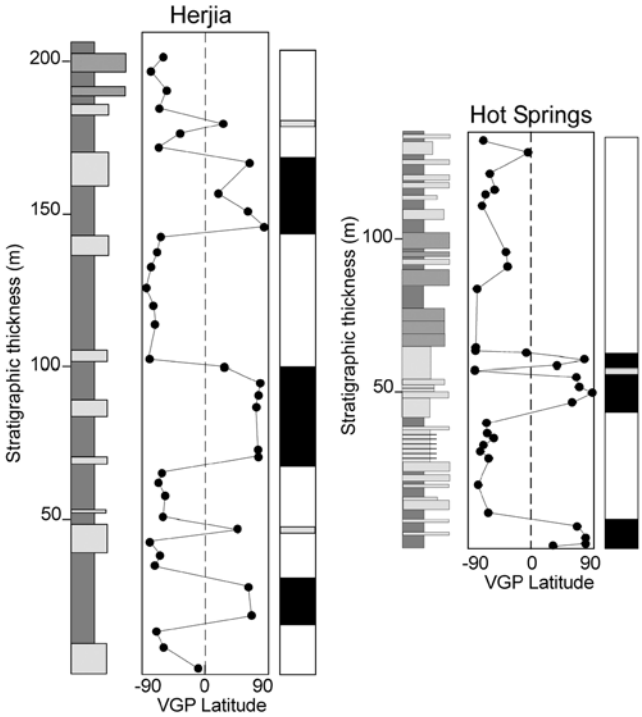

Figure 6. Plots of the virtual geomagnetic pole (VGP) latitudes versus lithostratigraphic position of sampling sites. For location of the stratigraphic sections see Figure 2.

tion in the Pliocene at about 3.5 to 3.8 Ma. Unfortunately, our magnetostratigraphy alone cannot resolve the question of whether this increased erosion and sedimentation is due to uplift or to climate change or both. Nonetheless, the unambiguous folding of, and thrusting onto, Late Miocene sediments (our own observations in the field) are suggestive of significant tectonic shortening at that time, indicating that post-Miocene uplift likely was a major factor.

6. Discussion and Conclusions

[26] Magnetic stratigraphy reveals that the main body of the sedimentary infilling (the Guide formation) in the eastern part of the Guide Basin is Pliocene in age. The presence of *Hipparion fossatum* [*Pan*, 1994] suggests that the onset of sedimentation to the east may have occurred in the Late Miocene or perhaps Middle Miocene and further magnetic stratigraphy is required to test that proposal. Overall, high-resolution magnetic stratigraphy in the basins of northern Tibet shows molasse deposition during enhanced denudation in the Pliocene. As we have seen earlier, the Qaidam basin, west of Guide, also shows the development of molasse type sediments in the Pliocene. Collectively, deposition of thick conglomerates around northern Tibet (Xiyu, Jishi, Ganjia gravels) reflects an enhanced depositional pulse in the mid-Pliocene. Our present data from the area of Guide, when combined with existing paleomagnetic studies from Linxia and Qaidam, indicate that development of the Guide–Gonghe, Qaidam, Linxia and Xining basins appears to be linked to reactivation of the Kunlun fault system to the south [*Burchfiel and Royden*, 1991; *Meyer et al.*, 1998; *Yin and Harrison*, 2000]. Deformation along the margins of the Guide–Gonghe basin can be explained by a transpressional setting, where thrusts coalesce with the major strike-slip faults such as the Kunlun and Qilian Shan fault systems. This model is compatible with the ideas of *Métivier et al.* [1998] in that the aggregate of basins around the northeastern rim of Tibet can best be envisioned as an amalgam of foreland depressions closely related to propagation of surrounding major faults (Altyn Tagh, Kunlun and Qilian) rather than as a continuum.

[27] Increased sediment flux and contractional deformation in the Tibetan Plateau are not restricted to the Pliocene though. Recent studies show indeed that during the Paleogene there was significant shortening, accommodated by both thrusting and right-slip faulting in Eastern Tibet [*Horton et al.*, 2000; *Spurlin et al.*, 2000]. Sedimentary records, growth strata and igneous activity lead to the suggestion that in the area of Nangqian-Yushu, in Eastern Tibet, a shift from thrusting to right-slip faulting occurred in the Paleogene, which could indicate a change in the state of stress field in Eastern Tibet [*Spurlin et al.*, 2000]. Around the margins of the Tarim basin, numerous studies also reveal the significance of uplift in the early Paleogene. P. E. Rumelhart et al. (The uplift of the northern Tibetan Plateau as recorded in the Cenozoic stratigraphy of Southern Tarim, Northwestern China, submitted to *Geological Society of America Bulletin*) infer an Oligocene age for the initial uplift, based on an integrated field-based study. In the same line of results, a recent magnetostratigraphic study by *Gilder et al.* [2001] carried out in the Subei basin, SE to the Altyn Tagh fault, reveals a thick pile of detrital sedimentary rocks ranging from the uppermost Oligocene to Lower Miocene in age. Increases in sedimentation and tectonic shortening in Subei reflect thrusts splaying from

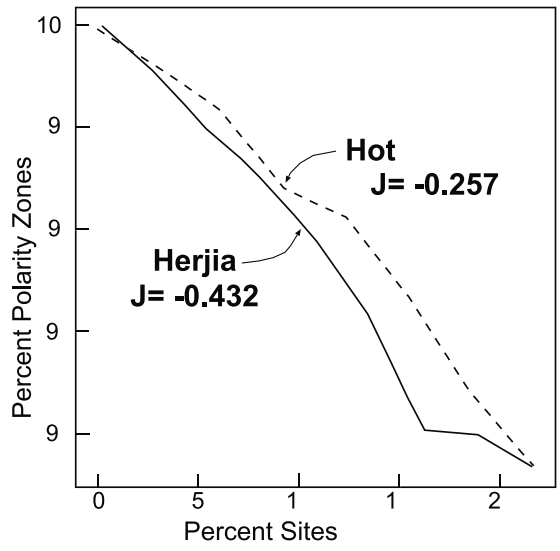

Figure 7. Magnetostratigraphic jackknife analysis [from *Tauxe and Gallet*, 1991] for the studied sections. The plot indicates the relationship between average percent of polarity zones retained and the percentage of sampling sites deleted [*Tauxe*, 1998]. The slope of the line gives the magnetostratigraphic jackknife parameter J. See text for details.

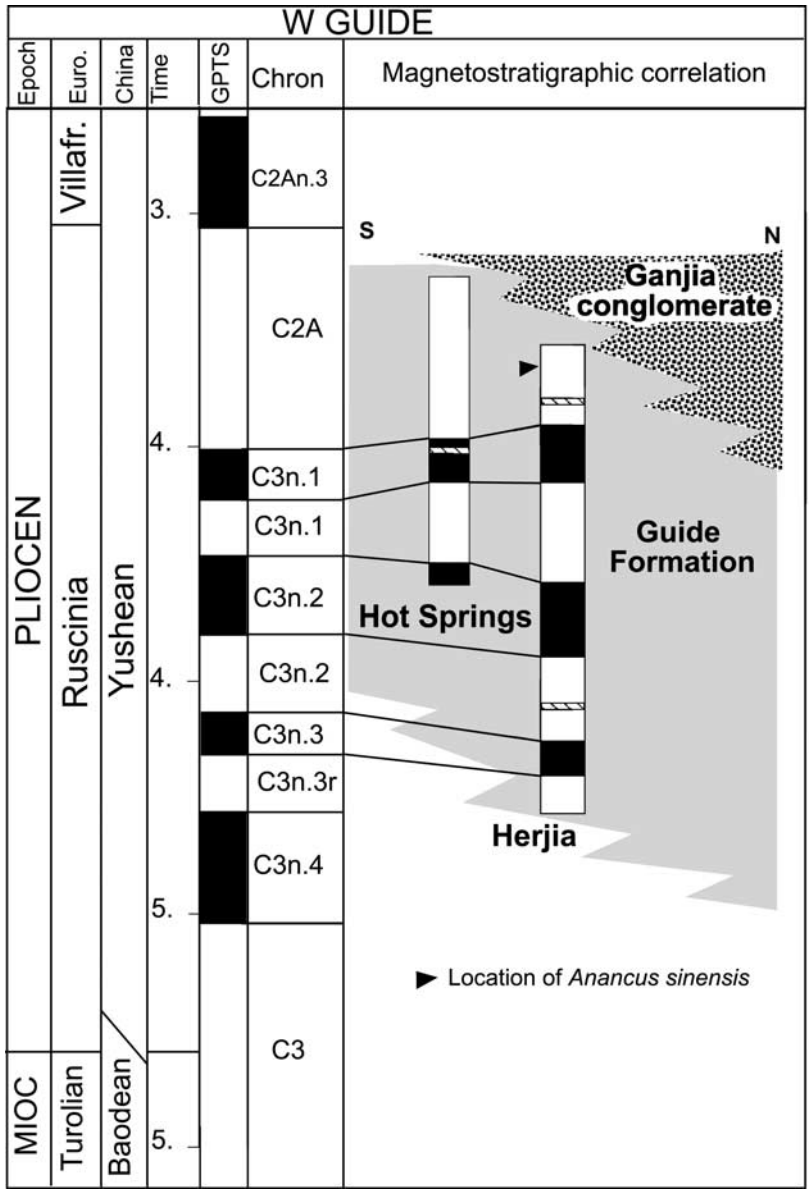

Figure 8. Correlation of the studied sections of the Guide formation to the Geomagnetic Polarity Time Scale [*Cande and Kent*, 1995]. Corresponding Chinese mammalian ages and epochs are shown. See text for discussion.

the Altyn Tagh fault in the Oligocene–Miocene [*Gilder et al.*, 2001; *Van der Woerd et al.*, 2001].

[28] The magnetostratigraphy of the intramontane Guide Basin, NE Tibet, defines the age of molasse sedimentary infilling. Paleomagnetic results reveal depositional ages of between 4.7 and 3.8 Ma for the middle part of the Guide formation and an average sedimentation rate of ~22 cm/kyr in the Pliocene, which is likely related to tectonic uplift and possibly strengthened by favorable climate conditions. Younger and older strata need to be further investigated with magnetostratigraphy. Thick conglomerates appear at about 3.8 Ma in the basin and likely reflect local thrusting and uplift in the surrounding mountain ranges.

[29] Further, this study emphasizes that uplift in the Tibetan plateau is a diachronous process. Several lines of evidence have suggested that uplift of southern Tibet occurred in the Miocene [*Copeland et al.*, 1987; *Harrison et al.*, 1993; *Coleman and Hodges*, 1995; *Garzione et al.*, 2000; *Williams et al.*, 2001]. In contrast, in Guide, northeastern Tibet, if the high sedimentation rates are mostly due to tectonism, then significant uplift occurred as late as Pliocene.

[30] **Acknowledgments.** This work was supported by the NSF Grant EAR9903074. The Scott Turner Fund, Department of Geological Sciences, University of Michigan provided fieldwork support. We thank R. Butler, J. Geissman and the Associate Editor for critically reading the manuscript and providing useful criticisms and comments.

References

Bally, A., I. M. Chou, R. Clayton, H. Eugester, and K. S. Meckel, Notes on sedimentary basins in China—Report of the American sedimentary delegation to the People's Republic of China, *Open File Rep. 86-327*, U.S. Geol. Surv., 1986.

Burchfiel, B. C., and L. H. Royden, Tectonics of Asia 50 years after the death of Emile Argand, *Eclogae Geol. Helv.*, *84*, 599–629, 1991.

Burchfiel, B. C., P. Molnar, Z. Zhao, K. Linag, and S. Wang, et al., Geology of the Ulugh Muztagh area, northern Tibet, *Earth Planet. Sci. Lett.*, *94*, 57–70, 1989.

Burchfiel, B. C., P. Zhang, Y. Wang, W. Zhang, F. Song, Q. Deng, P. Molnar, and L. Royden, Geology of the Haiyuan fault zone, Ningxia-Hui autonomous region, China, and its relation to the evolution of the northeastern margin of the Tibetan Plateau, *Tectonics*, *10*, 1091–1110, 1991.

Cande, S. C., and D. V. Kent, Revised calibration of the geomagnetic polarity timescale for the Late Cretaceous and Cenozoic, *J. Geophys. Res.*, *100*, 6093–6095, 1995.

Chen, Z., B. C. Burchfield, Y. Liu, R. W. King, L. H. Royden, W. Tang, E. Wang, J. Zhao, and X. Zhang, Global Positioning System measurements from eastern Tibet and their implications for India/Eurasia intercontinental deformation, *J. Geophys. Res.*, *105*, 16,215–16,227, 2000.

Coleman, M. E., and K. V. Hodges, Evidence for Tibetan Plateau uplift before 14 Myr ago from a new minimum estimate for east–west extension, *Nature*, *372*, 49–52, 1995.

Copeland, P. H., T. M. Harrison, W. S. F. Kidd, X. Ronghua, and Z. Yuquan, Rapid early Miocene acceleration of uplift in the Gangdese belt, Xizang (southern Tibet), and its bearing on accommodation mechanisms of the India–Asia collision, *Earth Planet. Sci. Lett.*, *86*, 240–252, 1987.

Dupont-Nivet, G., R. F. Butler, A. Yin, and X. Chen, Paleomagnetism indicates no Neogene rotation of the Qaidam Basin in northern Tibet during Indo-Asian collision, *Geology*, *30*, 263–266, 2002.

Einsele, G., *Sedimentary Basins, Evolution, Facies, and Sediment Budget*, 792 pp., Springer-Verlag, New York, 2000.

Flynn, L. J., Late Neogene mammalian events in north China, in *Actes du Congrès BiochroM'97*, *Mém. Trav. E.P.H.E. Inst. Montpellier*, vol. 21, edited by J. P. Aguilar, S. Legendre, and J. Michaux, pp. 183–192, 1997.

Flynn, L. J., W. R. Downs, N. Opdyke, K. Huang, and E. Lindsay, et al., Recent advances in the small mammal biostratigraphy and magnetostratigraphy of Lanzhou Basin, *Chin. Sci. Bull.*, *44*, 105–118, 1999.

Fothergill, P. A., Late Tertiary and Quaternary intermontane basin evolution in North-East Tibet: The Guide Basin, Ph.D. thesis, 228 pp., Univ. of London, 1998.

Fothergill, P. A., and H. Ma, Preliminary observations on the geomorphic evolution of the Guide Basin, Qinghai Province, China: Implications for the uplift of the northeast margin of the Tibetan Plateau, in *Uplift, Erosion and Stability: Perspectives on Long-Term Landscape Development*, *Geol. Soc. London Spec. Publ.*, vol. 162, edited by B. J. Smith, W. B. Whalley, and P. A. Warke, pp. 183–200, 1999.

Garzione, C. N., D. L. Dettman, J. Quade, P. G. DeCelles, and R. F. Butler, High times on the Tibetan Plateau: Paleoelevation of the Thakkhola graben, Nepal, *Geology*, *28*, 339–342, 2000.

Gilder, S., C. Yan, and S. Sen, Oligo-Miocene magnetostratigraphy and rock magnetism of the Xishuigou section, Subei (Gansu Province, western China) and implications for shallow inclinations in central Asia, *J. Geophys. Res.*, *106*, 30,505–30,522, 2001.

Gu, Z., S. Bai, X. Zhang, Y. Ma, S. Wang, and B. Li, Neogene subdivision and correlation of sediments within the Guide and Hualong basins of Qinghai province (in Chinese), *J. Stratigr.*, *16*, 96–104, 1992.

Harrison, T. M., P. Copleand, S. A. Hall, J. Quade, and S. Burner, et al., Isotopic preservation of Himalayan/Tibetan uplift, denudation, and climate histories of two molasse deposits, *J. Geol.*, *101*, 157–175, 1993.

Holt, W. E., N. Chamot-Rooke, X. Le Pichon, A. J. Haines, B. Shen-Tu, and J. Ren, Velocity field in Asia inferred from Quaternary fault slip rates and Global Positioning System observations, *J. Geophys. Res.*, *105*, 9,185–9,209, 2000.

Horton, B. K., A. Yin, M. Spurlin, J. Zhou, and J. Wang, Paleogene syncontractional sedimentary basins in the Eastern Tibetan Plateau, *Eos Trans. AGU*, *81*, Fall Meet. Suppl., F1083, 2000.

Kirschvink, J. L., The least-squares line and plane and the analysis of paleomagnetic data, *Geophys. J. R. Astron. Soc.*, *62*, 699–718, 1980.

Li, J. J., et al., Late Cenozoic magnetostratigraphy (11–0 Ma) of the Dongshanding and Wangjiashan sections in the Longzhong Basin, western China, *Geol. Mijnbouw*, *76*, 121–134, 1997a.

Li, J. J., X. M. Fang, R. Van der Voo, J. J. Zhu, C. MacNiocaill, Y. Ono, B. T. Pan, W. Zhong, and J. L. Wang, et al., Magnetostratigraphic dating of river terraces: Rapid and intermittent incision by the Yellow River of the northeastern margin of the Tibetan Plateau during the Quaternary, *J. Geophys. Res.*, *102*, 10,121–10,132, 1997b.

Li, J. J., X. M. Fang, Y. Ma, and A. D. Pan, in *Uplift and Environmental Changes of Qinghai–Xizang Plateau in Late Cenozoic* edited by Y. F. Shi, J. J. Li, and B. Y. Li, pp. 17–74, Guangdong Sci. and Technol., Guangzhou, 1998.

Liu, T., M. Ding, and E. Derbyshire, Gravel deposits on the margins of the Qinghai–Xizang Plateau, and their environmental significance, *Palaeogeogr. Palaeoclimatol. Palaeoecol.*, *120*, 159–170, 1996.

Liu, Z. C., Y. Wang, Y. Chen, X. Li, and Q. Li, Magnetostratigraphy and sedimentologically derived geochronology of the Quaternary lacustrine deposits of a 3000 m thick sequence in the central Qaidam basin, western China, *Palaeogeogr. Palaeoclimatol. Palaeoecol.*, *140*, 459–473, 1998.

Lyon-Caen, H., and P. Molnar, Gravity anomalies, flexure of the Indian plate, and the structure, support and evolution of the Himalaya and the Ganga Basin, *Tectonics*, *4*, 513–538, 1985.

McElhinny, M., *Paleomagnetism and Plate Tectonics*, Cambridge Univ. Press, New York, 1973.

Métivier, F., Y. Gaudemer, P. Tapponnier, and B. Meyer, Northeastward growth of the Tibet Plateau deduced from balanced reconstruction of two depositional areas: The Qaidam and Hexi Corridor basins, China, *Tectonics*, *17*, 823–842, 1998.

Meyer, B., P. Tapponnier, L. Bourjot, F. Métivier, Y. Gaudemer, G. Peltzer, S. GuoM, and Z. Chen, Crustal thickening in Gansu–Qinghai, lithospheric mantle subduction, and oblique, strike-slip controlled growth of the Tibet plateau, *Geophys. J. Int.*, *135*, 1–47, 1998.

Miall, A. D., Tectonic setting and syndepositional deformation of molasse and other nonmarine-paralic sedimentary basins, *Can. J. Earth Sci.*, *15*, 1613–1632, 1978.

Owen, L. A., Quaternary lacustrine deposits in a high energy semi-arid mountain environment, Karakoram Mountains, northern Pakistan, *J. Quat. Sci.*, *11*, 461–483, 1996.

Pan, B., Research upon geomorphologic evolution of the Guide Basin and the development of the Yellow River, *Arid Land Geogr.*, *7*(3), 43–50, in Chinese, 1994.

Pan, G., P. Wang, Y. Xu, S. Jiao, and T. Xiang, *Cenozoic Tectonic Evolution of Qinghai–Xizang Plateau* (in Chinese), *P. R. China Minist. of Geol. and Miner. Resour., Geol. Mem. Ser.*, vol. 5, no. 9, Geological Publ. House, Beijing, 1990.

Qinghai Geology Bureau, Geological map of Gou Ma Ying, scale 1:200.000, Xining, China, 1972.

Qiu, Z. X., and Z. D. Qiu, Chronological sequence and subdivision of Chinese Neogene mammalian faunas, *Palaeogeogr. Palaeoclimatol. Palaeoecol.*, *116*, 41–70, 1995.

Royden, L. H., and B. C. Burchfiel, The Tibetan Plateau and surrounding regions, in *Earth Structure: An Introduction to Structural Geology and Tectonics*, edited by B. van der Pluijm and S. Marshak, pp. 416–423, McGraw-Hill, New York, 1997.

Spurlin, M., A. Yin, M. Harrison, B. K. Horton, J. Zhou, and J. Wang, Two phases of Cenozoic deformation in East-central Tibet: Thrusting followed by right-slip faulting, *Eos Trans. AGU*, *81*, Fall Meet. Suppl., F1092, 2000.

Stober, J. C., and R. Thompson, Palaeomagnetic secular variation studies of Finnish lake sediment and the carriers of remanence, *Earth Planet. Sci. Lett.*, *37*, 139–149, 1977.

Tapponnier, P., et al., Active thrusting and folding in the Qi Lian Shan, and decoupling between the upper crust and mantle in northeastern Tibet, *Earth Planet. Sci. Lett.*, *97*, 382–403, 1990.

Tauxe, L., *Paleomagnetic Principles and Practice*, 299 pp., Kluwer Acad., Norwell, Mass., 1998.

Tauxe, L., and Y. Gallet, A jackknife for magnetostratigraphy, *Geophys. Res. Lett.*, *18*, 1783–1786, 1991.

Van der Woerd, J., F. J. Ryerson, P. Tapponnier, Y. Gaudemer, R. Finkel, M. Meriaux, Z. Caffee, H. Guoguang, and H. Qunlu, Holocene left-slip rate determined by cosmogenic surface dating on the Xidatan segment of the Kunlun fault (Qinghai, China), *Geology*, *26*, 695–698, 1998.

Van der Woerd, J., X. Xu, H. Li, P. Tapponnier, B. Meyer, F. J. Ryerson, A. S. Meriaux, and Z. Xu, Rapid active thrusting along the northwestern range front of the Tanghe Nan Shan (western Gansu, China), *J. Geophys. Res.*, *106*, 30,475–30,504, 2001.

Wang, E., Displacement and timing along the northern strand of the Altyn Tagh fault zone, northern Tibet, *Earth Planet. Sci. Lett.*, *150*, 55–64, 1997.

Wang, Q., et al., Present-day crustal deformation in China constrained by Global Positioning System measurements, *Science*, *294*, 574–577, 2001.

Williams, H., S. Turner, S. Kelley, and N. Harris, Age and composition of dikes in Southern Tibet: New constraints on the timing of east–west extension and its relationship to postcollisional volcanism, *Geology*, *29*, 339–342, 2001.

Yin, A., and T. M. Harrison, Geologic evolution of the Himalayan–Tibetan orogen, *Annu. Rev. Earth Planet. Sci.*, *28*, 211–280, 2000.

Zhai, Y., and T. Cai, The Tertiary system of Gansu Province, in *Gansu Geology* (in Chinese), People's Press of Gansu, pp. 1–40, 1984.

Zhang, P., B. C. Burchfiel, P. Molnar, W. Zhang, D. Jiao, Q. Deng, L. Royden, and F. Song, Amount and style of late Cenozoic deformation

in the Liupan Shan, Ningxia Autonomous Region, China, *Tectonics*, *10*, 111–1129, 1991.

Zhang, P., P. Molnar, and W. R. Downs, Increased sedimentation rates and grain sizes 2–4 Myr ago due to the influence of climate change on erosion rates, *Nature*, *410*, 891–897, 2001.

Zheng, H., C. M. Powell, Z. An, J. Zhou, and G. Dong, Pliocene uplift of the northern Tibetan Plateau, *Geology*, *28*, 715–718, 2000.

Zheng, S., W. Wu, Y. Li, and G. Wang, Late Cenozoic mammalian faunas from the Guide and Gonghe basins, Qinghai Province, *Vertebrata PalAsiatica*, *23*, 89–134, in Chinese, 1985.

Zhou, Z. Y., and P. J. Chen (Eds.), *Biostratigraphy and Geological Evolution of Tarim Basin: Beijing, China*, 439 pp., Science, Enfield, N. H., 1990.

Zijderveld, J. A. C., Demagnetization of rocks: Analysis of results, in *Methods in Paleomagnetism*, edited by D. Collinson, K. Creer, and S. Runcorn, pp. 254–286, Elsevier Sci., New York, 1967.

W. R. Downs, Department of Geology, Northern Arizona University, Flagstaff, AZ 86011-4099, USA.

X. Fang, Department of Geography, Lanzhou University, Gansu 730000, China.

J. M. Pares, R. Van der Voo, and M. Yan, Department of Geological Sciences, University of Michigan, 2534 C.C. Little Building, Ann Arbor, MI 48109, USA. (jmpares@umich.edu)